

# Chimeras in an adaptive neuronal network with burst-timing-dependent plasticity

Zhen Wang<sup>a</sup>, Sara Baruni<sup>b</sup>, Fatemeh Parastesh<sup>b</sup>, Sajad Jafari<sup>b</sup>, Dibakar Ghosh<sup>c,\*</sup>, Matjaž Perc<sup>d,e,f</sup>, Iqtadar Hussain<sup>g</sup>

<sup>a</sup> Shaanxi Engineering Research Center of Controllable Neutron Source, School of Science, Xijing University, Xi'an 710123, PR China

<sup>b</sup> Department of Biomedical Engineering, Amirkabir University of Technology, No. 350, Hafez Ave, Valiasr Square, Tehran 159163-4311, Iran

<sup>c</sup> Physics and Applied Mathematics Unit, Indian Statistical Institute, Kolkata 700108, India

<sup>d</sup> Faculty of Natural Sciences and Mathematics, University of Maribor, Koroška cesta 160, 2000 Maribor, Slovenia

<sup>e</sup> Department of Medical Research, China Medical University Hospital, China Medical University, Taichung, Taiwan

<sup>f</sup> Complexity Science Hub Vienna, Josefstadtstraße 39, 1080 Vienna, Austria

<sup>g</sup> Department of Mathematics, Statistics and Physics, Qatar University, Doha 2713, Qatar

## ARTICLE INFO

### Article history:

Received 10 January 2020

Revised 11 March 2020

Accepted 24 March 2020

Available online 29 April 2020

Communicated by Dr. Muhammet Uzuntarla

### Keywords:

Chimera state

Neuronal network

Adaptive coupling

Burst-timing-dependent plasticity

## ABSTRACT

The synchronized behavior of neurons depends on the structure and function of the synaptic connections between them. One of the activity-dependent synaptic modifications is the burst-timing-dependent plasticity, which relies on the latencies of the presynaptic and postsynaptic bursts. In this paper, we, therefore, study the collective behavior of a neuronal network with burst-timing-dependent plasticity, in particular, focusing on the emergence of chimera states. We consider separately non-local and global couplings, which have substantial effects on the collective dynamics. We show that the considered burst-timing-dependent plasticity leads to different behavior from static networks. The histogram of the synaptic strengths, in particular, reveals a different evolution of the chimera states in comparison to the development of synchronous and asynchronous states.

© 2020 Elsevier B.V. All rights reserved.

## 1. Introduction

Plasticity, which is defined as the variations in the synaptic strength and connections, or the excitability of the neurons, plays an essential role in the nervous system [1,2]. It has been revealed that during different neural behaviors such as the transitions between sleep and wakeful activity, the synapses experience short- and long-term changes [1]. The activities of the pre- and post-synapses can lead to either strengthening (potentiation) or weakening (depression) of the synaptic strength, lasting for short times, i.e., over minutes, or long times, i.e., over hours or more [3]. The potentiation and the depression are the result of various origins, including changes in the release of neurotransmitters or the chemical concentration and heterogeneous spatial distribution of the neurotransmission in the dendrites [4,5]. The short- and long-term alternations of synapses are the necessary mechanisms for memory and learning processes [6–8]. A large number of

researches have been focused on the study of the synaptic changes to reveal the underlying process of learning and memory [9–11].

The studies have shown that the timing of the firing of the pre- and post-synaptic neurons affect the synaptic strength. However, plasticity can also be induced by the delivery of amines or neuropeptides [1]. Many theoretical and experimental studies have focused on understanding how these adaptive modifications happen in the synapses [2,12,13]. These studies have led to the presentation of some well-known synaptic plasticity, such as the Bienenstock Cooper and Munro model and spike-timing-dependent plasticity model. In 2007, Butts et al. [14] performed an in-vitro experiment on the lateral geniculate nucleus neurons by patch recordings and found a new synaptic model, named burst-timing-dependent plasticity. They found that the learning rule in the retinogeniculate synapses is dependent on the timing of the pre- and post-synaptic bursts, such that short latencies lead to potentiation and longer ones lead to depression. This plasticity model is irrespective of the firing order of pre- and post-synaptic bursts and has a seconds-long temporal window.

Recently, many studies have focused on the study of the dynamics of complex networks [15–19]. The properties of the complex networks, including self-organization, lead to the emergence

\* Corresponding author.

E-mail address: [dibakar@isical.ac.in](mailto:dibakar@isical.ac.in) (D. Ghosh).

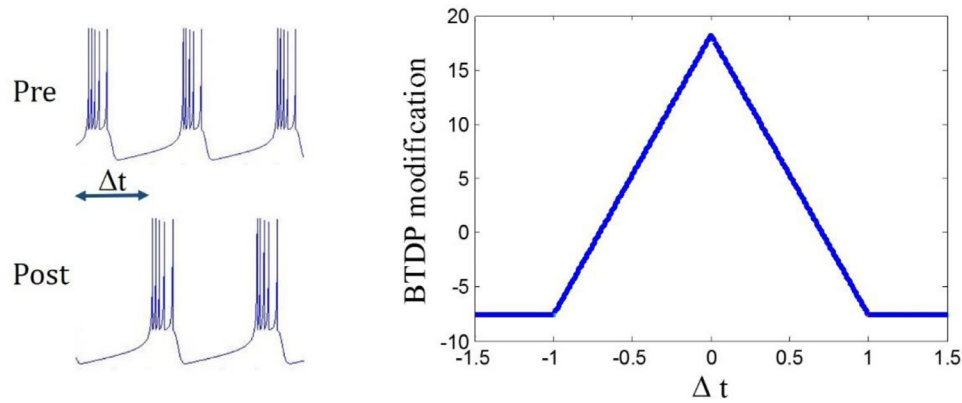


**Fig. 1.** The modification function of the burst-timing-dependent plasticity (BTDP). The synaptic weights are changed depending on the latency between the beginning times of the pre- and post-synaptic bursts.

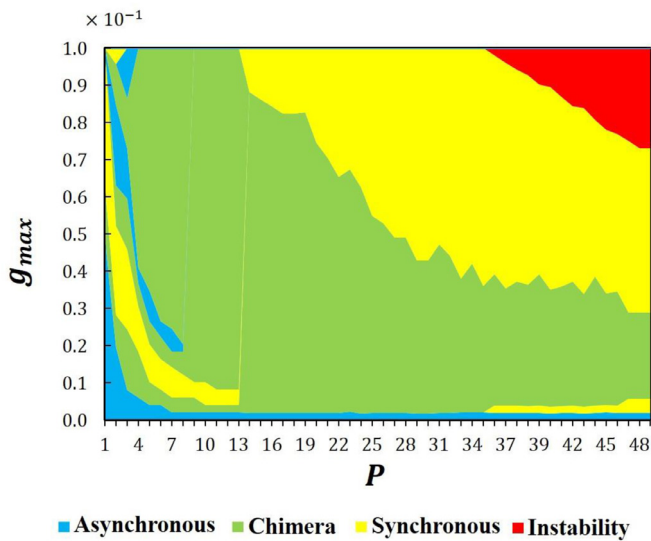


**Fig. 2.** Phase diagram of the network in  $(P, g_{max})$  plane with constant synaptic strength, showing different behaviors of the network. The blue, green, yellow and red colors show asynchronization, chimera state, synchronization, and instability regions, respectively. Here  $N = 100$  is the number of neurons in the network. The strength of incoherence is used to distinguish different states.

of different dynamical behaviors such as spiral waves, stochastic resonance, synchronization, etc. [20–23]. Synchronization is one of the crucial behaviors in many complex networks, including neuronal networks. Synchronization has been observed in different parts of the nervous system. It has been shown that synchronous activities of the neurons have essential importance in various neural processes, such as in cognitive tasks and information processing [24]. A majority of the recent researches has been devoted to the study of synchronization in neuronal networks [25–28]. In reality, neuronal networks are adaptive, and the synapses vary in time due to the neuromodulations and synaptic refinements [29]. Among the studies, a few have considered adaptive and time-varying networks. Some of the studies have focused on the synchronization of neuronal networks with time-varying structure [30,31], while some others have considered time-varying coupling strength [32]. For example, Rakshit et al. [31] explored synchronization in neuronal hypernetwork with electrical and chemical synapses, wherein the intralayer links were assumed to switch stochastically over time. Xie et al. [29] studied synchronization in a network of Hodgkin-Huxley neurons with spike-timing-dependent plasticity and inves-

tigated the effect of time delay. They found that the synchrony varies by increasing the plasticity rate, and there is an optimal rate at which the synchrony is the strongest.

The previous studies have led to the finding of many types of synchronization, including phase synchronization, lag synchronization, explosive synchronization, etc. [33,34]. In 2002, Kuramoto and Battogtokh [35] discovered a particular case, in which synchrony and asynchrony coexist in a network. This state, which was named chimera state [36], has attracted considerable attention in various scientific fields in recent years [37–40]. Since the chimera state is capable of describing the partial synchrony patterns, it is expected to be relevant with many brain functions. It has been suggested that chimera state has strong relations with uni-hemispheric sleep in some animals, during which, one part of the brain is sleep and synchronous, while the other part is awake and is asynchronous [41]. Furthermore, Andrzejak et al. [42] showed the similarities between chimera state collapses and epileptic seizures. Therefore, there have been many interests in the study of chimera states in neuronal networks [43–49]. Very recently, Bansal et al. [50] presented a cognitively informed framework with in-silico experiments and observed different patterns of synchronization, including chimeras. Calim et al. [51] investigated the emergence of chimera state in a network of non-locally coupled Morris-Lecar neurons exhibiting type-I excitability to provide a more realistic framework. Santos et al. [52] considered a network of Hindmarsh-Rose neurons with a connectivity matrix based on the cat cerebral cortex and demonstrated the existence of chimera-like states. Huo et al. [53] studied an adaptive neuronal network in which the coupling matrix was assumed to evolve with the dynamics of FitzHugh–Nagumo neurons and observed that the adaptive coupling could induce diverse chimera patterns.

In this paper, we consider a network of bursting neurons with burst-timing-dependent plasticity and study the emergence of chimera state. Firstly, we investigate the network with static coupling by varying the coupling parameters and find the conditions for the appearing of the chimera state. Then the effect of the burst-timing-dependent plasticity coupling on the collective behavior of the network is investigated. Since in this case, the synaptic strength is not static and varies in time, we refer to it as the adaptive coupling. Fig. 1 shows the modification function of the burst-timing-dependent plasticity. As Fig. 1 shows, this modification rule depends on the latency between the beginning times of the pre- and post-synaptic bursts. For smaller latencies, the synapse is potentiated, and for larger latencies, the synapse is depressed. Therefore, we study how the dynamical behaviors change using this burst timing-dependent plasticity in globally and locally coupled neurons in comparison to the static coupling. We

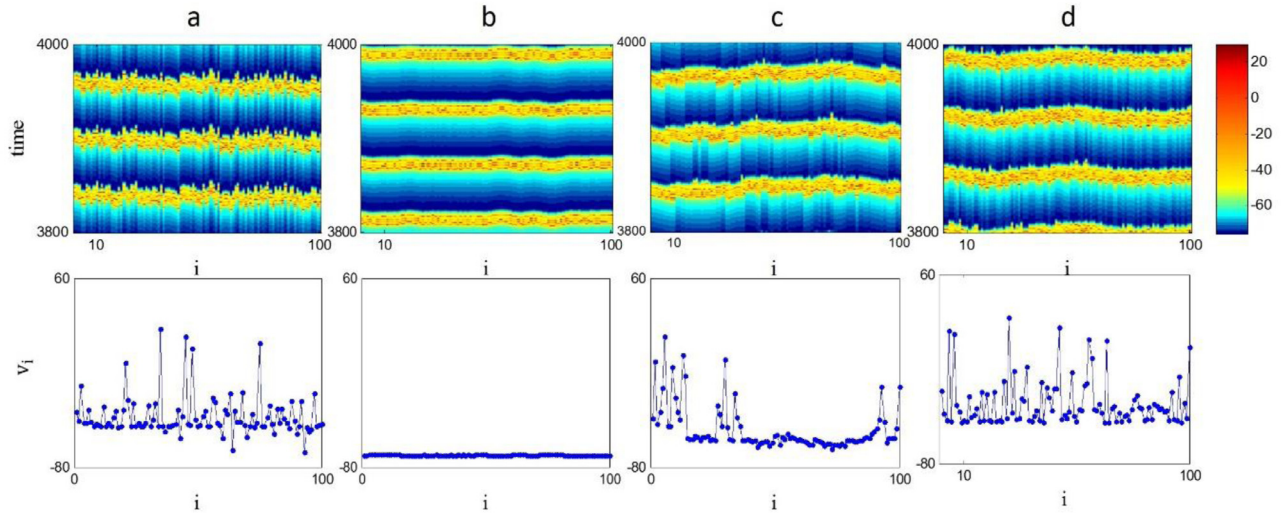


**Fig. 3.** Spatiotemporal patterns (first row) and the time snapshots (second row) of the static network for  $P=3$  and different coupling strengths, showing repetitive patterns. a) asynchronization for  $g_{max} = 0.002$ , b) synchronization for  $g_{max} = 0.026$ , c) chimera state for  $g_{max} = 0.039$ , d) asynchronization for  $g_{max} = 0.048$ .

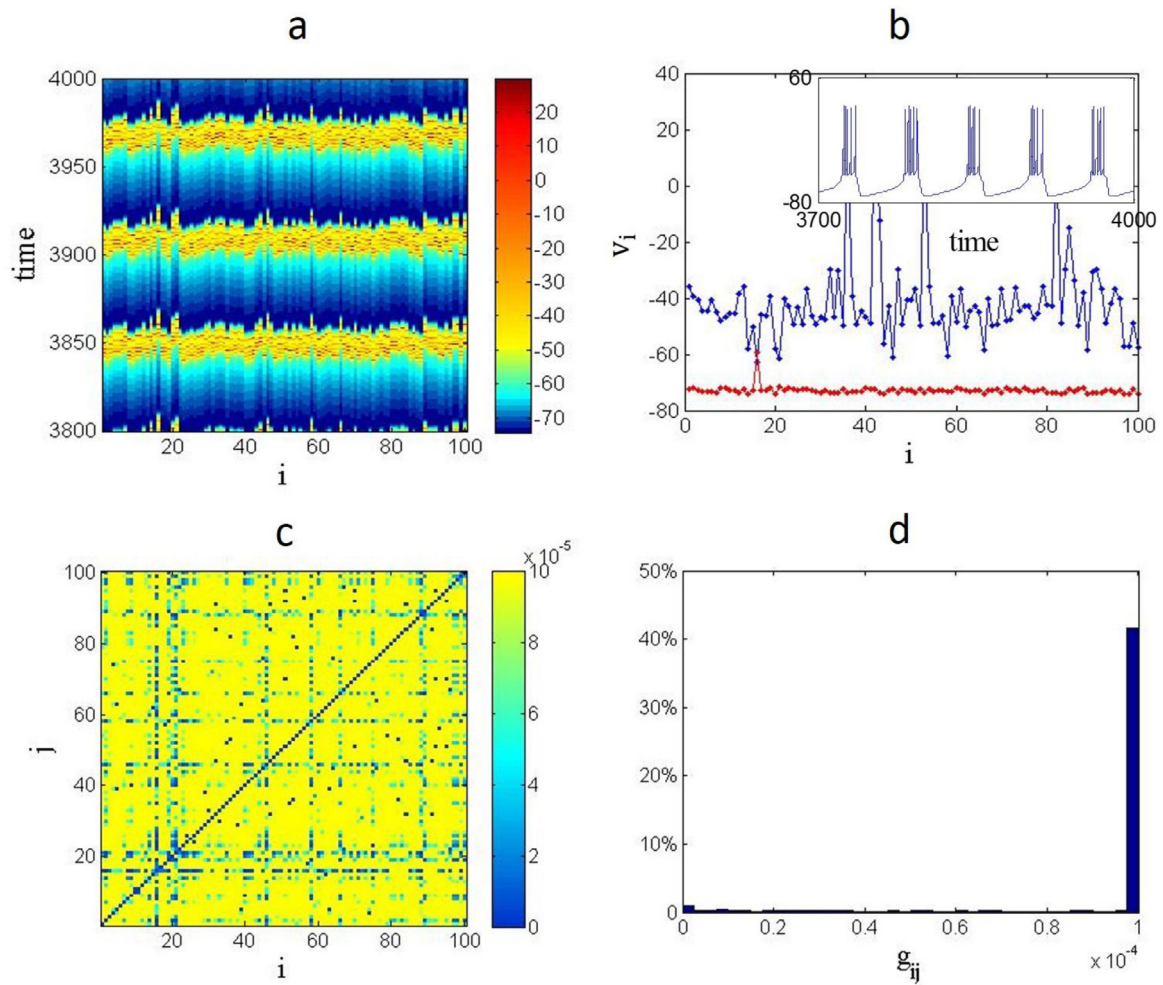


**Fig. 4.** The evolution of the globally coupled network with burst-timing-dependent plasticity rule for  $g_{max} = 0.0001$  showing asynchronous oscillations. a) Spatiotemporal pattern and b) the time snapshot of the membrane potential of the neurons. c) coupling matrix and d) histogram of the coupling matrix at  $t = 4000$ . For small coupling strength values, the network is asynchronous and about 42% of the coupling weights are at the maximum.



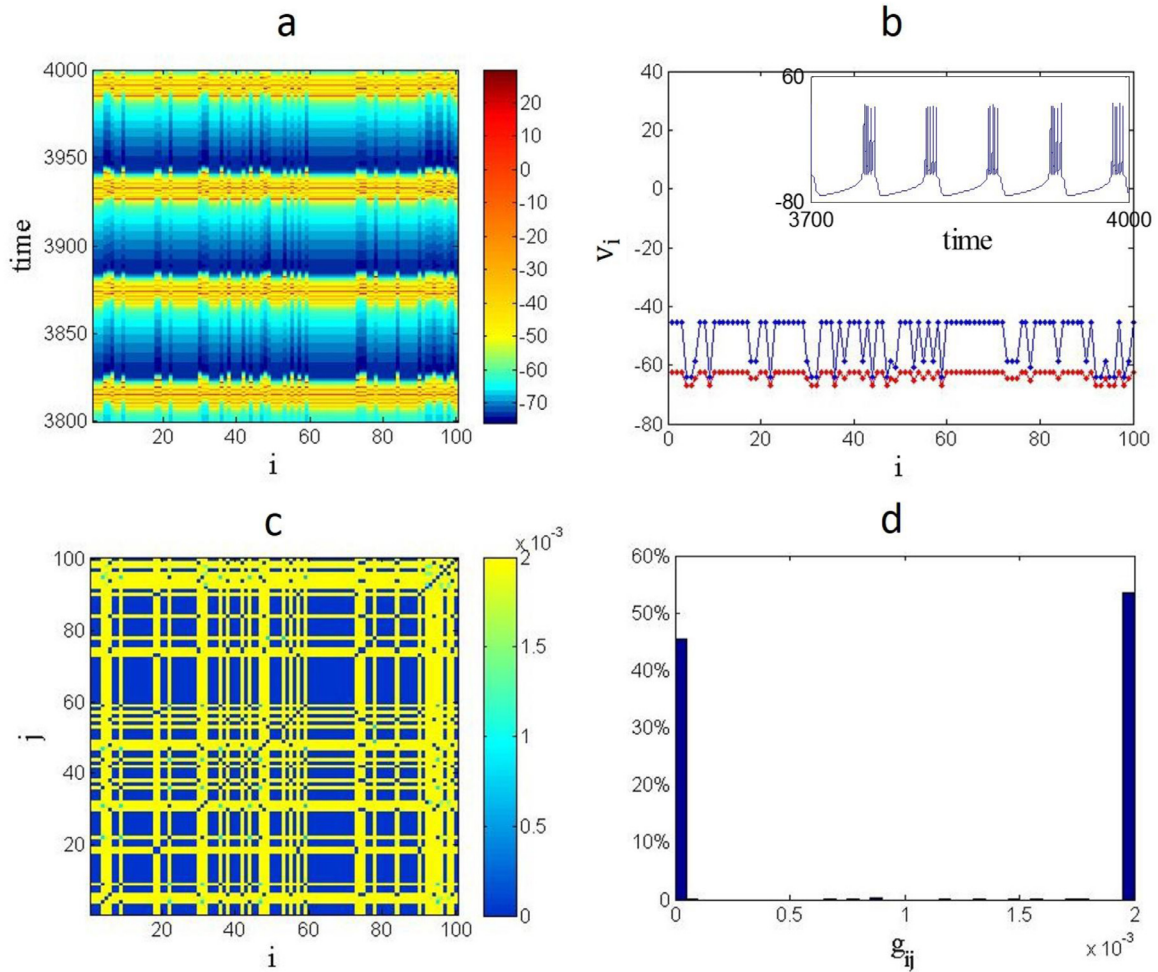


**Fig. 5.** The evolution of the globally coupled network with burst-timing-dependent plasticity rule for  $g_{max} = 0.002$  showing chimera state. a) Spatiotemporal pattern and b) the time snapshot of the membrane potential of the neurons. c) Coupling matrix and d) histogram of the coupling matrix at  $t = 4000$ . In specific coupling strength values, the network shows chimera state and about 53% of the coupling weights are at the maximum, while 45% are at the minimum.

observe that the synchronization of neurons occurs in high coupling strength for the burst-timing-dependent plasticity, while the chimera state emerges for static coupling. The different dynamical states are investigated by changing the synaptic strength and non-local parameter of the neuronal network. Finally, all the obtained states, namely asynchronous, synchronous, chimera and instability (i.e. unbounded state) are confirmed by plotting the spatiotemporal pattern, the snapshot of the membrane potential of the neurons, the coupling matrix and the histogram of the corresponding coupling matrix.

## 2. Model and methods

To study the behavior of the adaptively coupled neurons and the effects of the burst-timing-dependent plasticity, we consider the two-variable integrate-and-fire (IF) model of Izhikevich. The mathematical form of each unit of the network is as follows,

$$\begin{aligned} \dot{v}_i &= 0.04v_i^2 + 5v_i + 140 - u_i + I + I_i^{syn} \\ \dot{u}_i &= a(bv_i - u_i), \\ f \ v_i > 30\text{mv}, \text{ then } &\begin{cases} v_i \leftarrow c \\ u_i \leftarrow u_i + d \end{cases} \end{aligned} \quad (1)$$

where  $i = 1, 2, \dots, N$ , and  $N$  is the number of neurons in the network. The variables  $v$  and  $u$  represent the membrane potential of the neuron and its membrane recovery variable, respec-

tively. The parameters  $a, b, c$ , and  $d$  are constants and determine the behavior of the neuron.  $I$  represents the external current, and  $I_i^{syn}$  shows the synaptic current, which is obtained by the dynamics of the synaptic variable  $s_j$ :

$$\begin{aligned} I_i^{syn} &= - \sum_{j \neq i}^N g_{ji} C_{ji} s_j (v_i - v_{syn}), \\ \dot{s}_j &= \alpha(v_j)(1 - s_j) - s_j/\tau, \\ \alpha(v_j) &= \alpha_0 / (1 + e^{-v_j/v_{shp}}), \end{aligned} \quad (2)$$

where  $C_{ij}$  is the connectivity matrix with  $C_{ij} = 1$  if the  $i$ th neuron is connected with the  $j$ th neuron and  $C_{ij} = 0$  otherwise. Since all the synapses are considered excitatory, the reversal potential is set at  $v_{syn} = 0$ . When the pre-synaptic neuron is in the silent state ( $v_j < 0$ ),  $s_j$  can be approximated by  $\dot{s}_j = -\beta s_j$ . In other cases,  $s_j$  jumps quickly to 1 and acts on the post-synaptic neurons. Therefore, the synaptic recovery function  $\alpha(v)$  can be considered as the Heaviside function. Here,  $v_{shp}$  defines the threshold above which the post-synaptic neuron is affected by the pre-synaptic one and is set to  $v_{shp} = 0.05$ . The parameters are chosen as  $a = 0.02$ ,  $b = 0.2$ ,  $c = -50$ ,  $d = 2$ ,  $I = 10$ ,  $\alpha_0 = 2$ ,  $\beta = 1$ . The synaptic conductance  $g_{ji}$  from the  $j$ th to the  $i$ th neuron is updated through burst-timing-dependent plasticity modification function, which is as

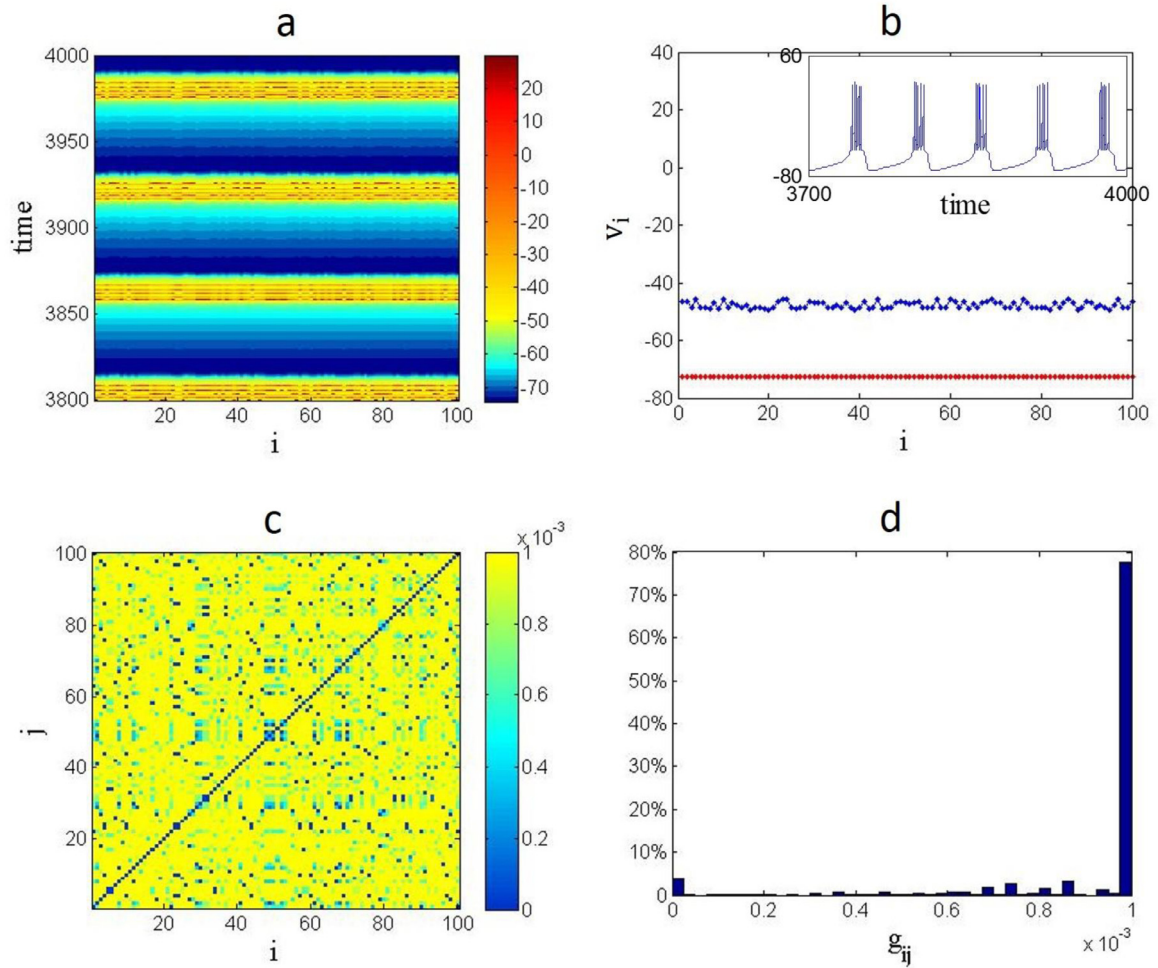


**Fig. 6.** The evolution of the globally coupled network with burst-timing-dependent plasticity rule for  $g_{max} = 0.001$  showing synchronous state oscillations. a) Spatiotemporal pattern and b) the time snapshot of the membrane potential of the neurons. c) Coupling matrix and d) histogram of the coupling matrix at  $t = 4000$ . For higher coupling strength values, the network becomes synchronous and about 78% of the coupling weights are at the maximum.

follows:

$$F(\Delta t) = \begin{cases} 18.2 - 25.8|\Delta t| & \text{if } |\Delta t| < 1, \\ -7.6 & \text{if } |\Delta t| \geq 1, \end{cases} \quad (\% s^{-1}) \quad (3)$$

where  $\Delta t = t_j - t_i$ , and  $t_j$  and  $t_i$  are the beginning times of the bursts of the postsynaptic and presynaptic neurons. With this modification function, the synaptic weights are updated and kept in  $[0, g_{max}]$ , with  $g_{max}$  being the upper limit.

For the numerical simulations, a ring network of the coupled neurons is considered with periodic boundary condition. The network is numerically solved by using the 4th order Runge–Kutta algorithm with selecting random initial conditions and the integration time-step of 0.01. In the following section, we will pursue the different dynamical behaviors using the burst-timing-dependent plasticity in the non-locally coupled neuronal network (1) together with (2). Our main emphasis here is to identify the parameter region by simultaneously changing the synaptic weights and the number of neighboring nodes  $P$ . Finally, we will compare the results of static and adaptive networks.

### 3. Results

At first, it is assumed that the coupling weights are not adaptive. The network is investigated by considering different coupling matrices from local to global connection and various synaptic strengths. The coupling matrix is constructed by the nearest

neighbor method, i.e.,  $C_{ij} = 1$  for  $i - P \leq j \leq i + P$  and  $C_{ij} = 0$  otherwise, where  $P$  is the number of neighboring nodes connected on both sides of the ring network. For each parameter values, the spatiotemporal patterns are obtained, and the behavior of the network is considered. Fig. 2 shows the phase diagram of the static network in  $(P, g_{max})$  plane, displaying the asynchronous state by blue, chimera state by green, synchronous state by yellow and instability (unbounded state) by red. To identify different states, we have used the strength of incoherence [54] as a measurement (for details, see Appendix). As the figure shows, for local coupling and non-local coupling with small  $P$ , the network transits between different states by increasing the synaptic strength. For  $19 < P < 35$ , the network exhibits chimera state in small coupling weights and raising the synaptic strength synchronizes the network. For higher  $P$  values, the network becomes unstable for large synaptic strengths.

Interestingly, the network exhibits repetitive patterns for low  $P$  values. Fig. 3 demonstrates the different behaviors of the network for  $P = 3$ . In this figure, the first row shows the spatiotemporal patterns, and the second row illustrates the time snapshots. Fig. 3a shows the asynchronous behavior of the neurons for  $g_{max} = 0.002$ , and Fig. 3b illustrates the synchronous motion of the neurons for  $g_{max} = 0.026$ . By further increasing the coupling strength, the synchronous behavior is disturbed, and the chimera state is observed, as shown in Fig. 3c. But this pattern is not stable, and raising the coupling strength leads to asynchronization of the neurons, as

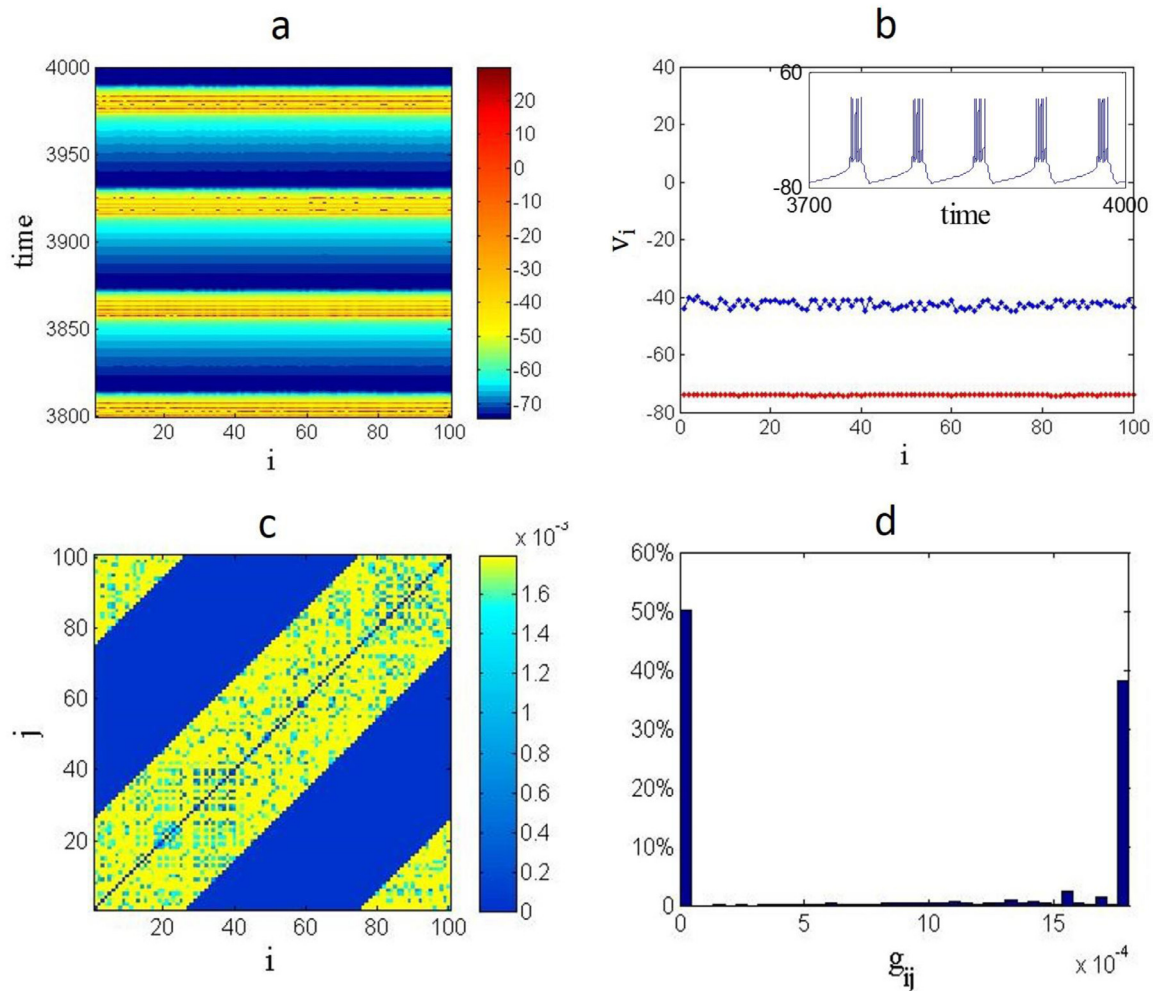


**Fig. 7.** The evolution of the non-locally coupled network ( $P = 25$ ) with burst-timing-dependent plasticity rule for  $g_{max} = 0.0018$  showing synchronization. a) Spatiotemporal pattern and b) the time snapshot of the membrane potential of the neurons. c) coupling matrix and d) histogram of the coupling matrix at  $t = 4000$ . Similar to the global coupling, about 75% of the adaptive couplings have reached the maximum.

shown in Fig. 3d. Fig. 2 depicts that such transitions between states also occur by increasing the coupling strength.

Next, the adaptive coupling is considered by using the burst-timing-dependent plasticity rule for the synaptic weights. The results show that by changing the coupling to the adaptive plasticity, the network behavior varies. Firstly, we examine the network in the case of global coupling. In this case, when the coupling strength is very small, the network is asynchronous until  $g_{max} = 0.0008$ . As  $g_{max}$  grows, some of the neurons intend to be synchronous, and thus, the network shows chimera state. By more increasing of  $g_{max}$ , all the oscillators become synchronous, such that the network is completely synchronous for  $0.001 < g_{max} < 0.002$ . Further increasing of the coupling upper limit ( $g_{max}$ ), returns the network state to chimera state. Subsequently, the network exhibits chimera state for  $0.0008 < g_{max} < 0.001$  and  $0.002 < g_{max} < 0.05$ .

The development of the network in different states is shown in Figs. 4–6. In these figures, subfigure-a is the spatiotemporal pattern of the network in which the membrane potential of the neurons is illustrated by color. Subfigure-b shows the time-snapshots of the membrane potential of the neurons. The time series of one neuron of the network is presented in the inset of subfigure-b. As it is observed from the time series, the dynamics consists of two stages of higher chaotic firing (the bursts) and the rest. To observe the state of the neurons, the time snapshot of the bursting stage is shown by

blue, and the time snapshot of the resting stage is shown by red. Subfigure-c demonstrates the evolution of the synaptic strengths, in which the weight of the synapse connecting neuron  $i$  to  $j$  is depicted by color. Finally, subfigure-d depicts the histogram of the synaptic strength at  $t = 4000$  time-units. Fig. 4 shows the network behavior in  $g_{max} = 0.0001$ , at which the neurons are asynchronous. Subfigures-a, b of this figure show the disordered state of the network. From subfigure-b, it is inferred that in both stages, the neurons are asynchronous, but the amplitude variations in the rest state are lower. The inset of subfigure-b shows that the behavior of all neurons in the asynchronous state is the square wave bursting. As time passes, the synapses of the network are modified, and finally, almost 42% of the weights are near the upper limit ( $g_{max}$ ).

Fig. 5 shows the network state for  $g_{max} = 0.002$ . The spatiotemporal pattern and the time snapshot of the network depict that the network is in chimera state for this coupling strength. The synaptic weights have been modified in a way that a group of neurons reaches a common motion. The blue and red time snapshots in subfigure-b show that the chimera state exists in both burst and rest stages. Furthermore, the behavior of the neurons is the square wave bursting, and the bursts in the synchronized groups are completely synchronized. Comparing the coupling matrix (Fig. 5c and d) with the previous asynchronous state (Fig. 4c and d) shows that in this case, approximately the coefficients have been divided into two groups of lower limit ( $g_{ij} = 0$ ) and upper limit



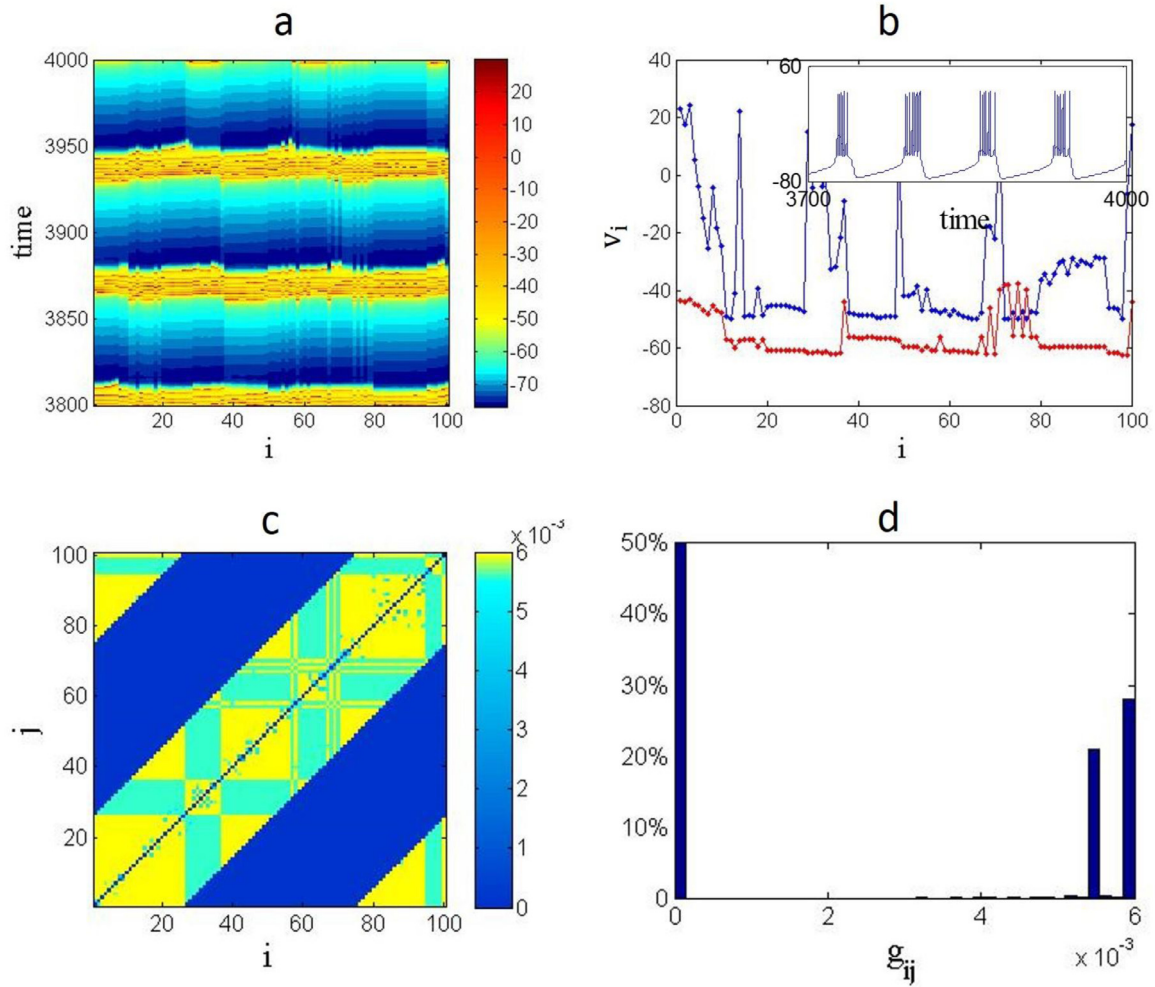


**Fig. 8.** The evolution of the non-locally coupled network ( $P = 25$ ) with burst-timing-dependent plasticity rule for  $g_{max} = 0.006$  showing chimera state. a) Spatiotemporal pattern and b) the time snapshot of the membrane potential of the neurons. c) coupling matrix and d) histogram of the coupling matrix at  $t = 4000$ . In the case of chimera state in non-local connection, a considerable number of coupling weights are between minimum and maximum.

( $g_{ij} = g_{max}$ ). It is worth mentioning that according to Fig. 2, this setting of the parameter values leads to the synchronized behavior of the static network. While in the adaptive coupling, the network is synchronous for  $0.001 < g_{max} < 0.002$ . The spatiotemporal pattern and the time snapshots of the synchronous network for  $g_{max} = 0.001$  are shown in Fig. 6a and b. Subfigure-b depicts that the neurons in the rest state are fully synchronized, while there are small alternations in the burst stage. However, the pattern is burst synchronization. The histogram of the coupling matrix in the synchronous state, which is demonstrated in Fig. 6d, shows that in this case, close to 80% of the synaptic weights have the upper limit value.

In the next step, we investigate the effect of burst-timing-dependent plasticity rule on the dynamics of a non-locally coupled network. In this case, each neuron is coupled to its  $2P$  nearest neighbors. Thus, the Laplacian matrix  $L$  for the nonlocal coupling is as follows:

$$L_{ij} = \begin{cases} 1, & 0 < |i - j| \leq P \\ -2P, & i = j \\ 0, & \text{otherwise} \end{cases} \quad (4)$$

We have selected a moderate value of  $P = 25$  for non-local coupling in our simulations. Generally, the obtained numerical results indicate different patterns in comparison to global coupling. Fig. 7 shows the network development for  $g_{max} = 0.0018$ , at which the network is synchronous. Since the coupling is non-local

with  $P = 25$ , just half of the synaptic weights have been updated through burst-timing-dependent plasticity, and half of the weights are zero (see Fig. 7c). Similar to the global coupling, near to 75% of the adaptive weights have reached the maximum possible weight ( $g_{max}$ ), and the remained 25% are distributed in other values below  $g_{max}$ . Here, the resting states of all the neurons are in synchrony. Moreover, the dynamics of the neurons is not changed by varying the coupling and is still the square wave bursting.

The pattern of the network for higher value of  $g_{max} = 0.006$  is demonstrated in Fig. 8. The spatiotemporal pattern and the time snapshot figure show the existence of the chimera state. In Fig. 8(b), the snapshots of burst (blue dotted line) and resting states (red dotted line) show the emergence of chimera behaviors. Here the behaviors of each neuron are in chaotic square-wave bursting. In this case, 56% of the adaptive weights have a value near  $g_{max} = 0.006$ , and 42% are near 0.0055, and the low remaining percentage is spread in the range  $[0.003 \ 0.006]$ .

To provide a comparative perspective between the emergent states in the static synaptic weight and the adaptive one with burst-timing-dependent plasticity rule, Fig. 9 is presented. In this chart, the dynamical behavior of the network in two cases of global and non-local coupling is represented for different  $g_{max}$  values. According to this figure, in the case of global coupling, when the synaptic weights are static, the chimera state exists for  $0.004 < g_{max} < 0.026$ , and for  $g_{max} > 0.026$ , the network becomes synchronous. But if the synapses are updated through

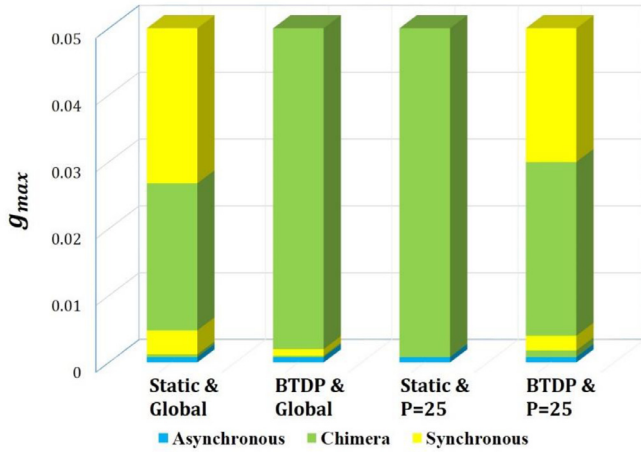


**Fig. 9.** The dynamical behavior of the network in different cases of global coupling with static or adaptive synapses (burst-timing-dependent plasticity (BTDP)) and non-local coupling with static or adaptive synapses (burst-timing-dependent plasticity), for  $g_{max}$  value in  $[0, 0.05]$ . The blue color shows where the network is asynchronous, the green shows chimera state and the yellow shows synchronization.

burst-timing-dependent plasticity, the synchronous state does not emerge by increasing  $g_{max}$ , and the chimera state appears for  $0.002 < g_{max} < 0.05$ . In the case of non-local coupling, the network behavior is inverse. Actually, in  $P = 25$ , when the synapses are static, the chimera states are observed for  $g_{max} > 0.0008$ . While the burst-timing-dependent plasticity is applied, the network exhibits synchronized behavior for  $g_{max}$  in the range  $[0.0018, 0.004]$  and  $[0.03, 0.05]$ . It should be noted that in the analysis of the adaptive network, we have investigated the network behavior until  $g_{max} = 0.05$  since it was observed that by adjusting  $g_{max} > 0.05$ , the neurons' firing patterns were converted from burst firing to spiking.

### 3. Discussion

The studies have shown that during different processes in the brain, the synapses are refined by either strengthening or weakening, which is called plasticity. In the studies, different plasticity rules have been proposed. Previous studies reveal that plasticity can affect the collective behavior of the neurons, such as synchronization. The burst-timing-dependent plasticity is a plasticity model, discovered in lateral geniculate nucleus neurons. In this paper, the emergence of the chimera state is investigated in an adaptive network of bursting neurons with the burst-timing-dependent plasticity model. At first, the network behavior is studied in the case of static coupling by varying the coupling strength and coupling range (the number of neighbors in coupling). Then the burst-timing-dependent plasticity is applied, and the network is investigated in two cases of non-local coupling and global coupling. When the neurons are globally coupled, in the case of synchronization and asynchronization, the synaptic weights are modified such that the majority of the synapses had reached the upper limit of the coupling strength. While when the chimera state emerged, nearly half of the weights has the upper limit value, and roughly half are set to zero. When the neurons are coupled non-locally, the synaptic weights are modified the same as the global coupling in the case of synchronization and asynchronization. But in the case of chimera states, the majority of the modifiable weights are strengthened near the upper limit. Overall, burst timing-dependent plasticity changed the dynamical behavior of the network such that in the global static coupling, the network is synchronous for high coupling strengths, but in the global adap-

tive coupling, the network could not become synchronous. For the non-local coupling, the network behavior is inverse. It is observed that burst-timing-dependent plasticity led to the synchronization of neurons in high coupling strengths, while in the static coupling, the chimera state emerged. Investigating the dynamics of the neurons showed that in all cases, the neurons exhibit square wave bursting, and this behavior is not varied by changing the coupling.

### Credit authors statement

ZW, SB, FP, SJ, DG, MP and IH designed and performed the research as well as wrote the paper.

### Declaration of Competing Interest

The authors declare that they have no conflict of interest.

### Acknowledgments

ZW was supported by the Natural Science Basic Research Plan in Shaanxi Province of China (grant number 2020JM-646), the Key Research and Development Program of Shaanxi (No. 2018GY-091, 2019GY-025), the Innovation Capability Support Program of Shaanxi (No. 2018GHJD-21), the Science and Technology Program of Xi'an (No. 2019218414GXRC020CG021-GXYD20.3). MP was supported by the Slovenian Research Agency (Grants J4-9302, J1-9112, and P1-0403).

### Appendix: Strength of incoherence

To characterize different dynamical behaviors of the network, a statistical measure is used. The strength of incoherence uses the time series of the network and computes the local standard deviation [54]. To calculate the strength of incoherence, firstly, the state variables are transformed into new variables  $w_i = v_i - v_{i+1}$ . Then the neurons are divided into  $M$  bins of equal length  $n = \frac{N}{M}$ , and the standard deviation of each bin is calculated as follows:

$$\sigma(m) = \sqrt{\frac{1}{n} \sum_{j=n(m-1)+1}^{nm} [w_j - \bar{w}]^2} \quad (5)$$

where  $\bar{w} = \frac{1}{N} \sum_{i=1}^N w_i$ , and  $m = 1, \dots, N$ . Then, the strength of incoherence (SI) is obtained by:

$$SI = 1 - \frac{\sum_{m=1}^M s_m}{M}, \quad s_m = \vartheta(\delta - \sigma(m)) \quad (6)$$

with  $\vartheta(\cdot)$  being the Heaviside step function, and  $\delta$  a predefined threshold. Consequently, the value of SI defines the level of network synchrony, such that the asynchronous, synchronous, and chimera states are characterized by  $SI = 1$ ,  $SI = 0$ , and  $0 < SI < 1$ , respectively.

### References

- [1] A. Destexhe, E. Marder, Plasticity in single neuron and circuit computations, *Nature* 431 (2004) 789.
- [2] N.C. Spitzer, Neurotransmitter switching? No surprise, *Neuron* 86 (2015) 1131–1144.
- [3] N. Deperrois, M. Graupner, Short-term depression and long-term plasticity together tune sensitive range of synaptic plasticity, *BioRxiv*, (2019) 565291.
- [4] M. Uzuntarla, J.J. Torres, P. So, M. Ozer, E. Barreto, Double inverse stochastic resonance with dynamic synapses, *Phys. Rev. E* 95 (2017) 012404.
- [5] M. Uzuntarla, M. Ozer, U. Ileri, A. Calim, J. Torres, Effects of dynamic synapses on noise-delayed response latency of a single neuron, *Phys. Rev. E* 92 (2015) 062710.
- [6] S. Schacher, J.-Y. Hu, The less things change, the more they are different: contributions of long-term synaptic plasticity and homeostasis to memory, *Learn. Memory* 21 (2014) 128–134.



- [7] S. Johnson, J. Marro, J.J. Torres, Robust short-term memory without synaptic learning, *PLoS One* 8 (2013) e50276.
- [8] L. Pantic, J.J. Torres, H.J. Kappen, S.C. Gielen, Associative memory with dynamic synapses, *Neural Comput.* 14 (2002) 2903–2923.
- [9] D. Buonomano, T.P. Carvalho, A novel learning rule for long-term plasticity of short-term synaptic plasticity enhances temporal processing, *Front. Integr. Neurosci.* 5 (2011) 20.
- [10] S. Meis, T. Endres, T. Munsch, V. Lessmann, The relation between long-term synaptic plasticity at glutamatergic synapses in the amygdala and fear learning in adult heterozygous BDNF-knockout mice, *Cereb. Cortex* 28 (2018) 1195–1208.
- [11] J. Artinian, J.-C. Lacaille, Disinhibition in learning and memory circuits: new vistas for somatostatin interneurons and long-term synaptic plasticity, *Brain Res. Bull.* 141 (2018) 20–26.
- [12] V. Delattre, D. Keller, M. Perich, H. Markram, E.B. Muller, Network-timing-dependent plasticity, *Front. Cell. Neurosci.* 9 (2015) 220.
- [13] A. Fachechi, E. Agliari, A. Barra, Dreaming neural networks: forgetting spurious memories and reinforcing pure ones, *Neural Netw.* 112 (2019) 24–40.
- [14] D.A. Butts, P.O. Kanold, C.J. Shatz, A burst-based “Hebbian” learning rule at retinogeniculate synapses links retinal waves to activity-dependent refinement, *PLoS Biol.* 5 (2007) e61.
- [15] Ö.N. Yaveroğlu, N. Malod-Dognin, D. Davis, Z. Levnajic, V. Janjic, R. Karapandza, A. Stajmirovic, N. Pržulj, Revealing the hidden language of complex networks, *Sci. Rep.* 4 (2014) 4547.
- [16] Z.-K. Gao, M. Small, J. Kurths, Complex network analysis of time series, *EPL* 116 (2017) 50001.
- [17] Z. Levnajic, A. Pikovsky, Untangling complex dynamical systems via derivative-variable correlations, *Sci. Rep.* 4 (2014) 5030.
- [18] Z.-K. Gao, N.-D. Jin, A directed weighted complex network for characterizing chaotic dynamics from time series, *Nonlinear Anal. Real World Appl.* 13 (2012) 947–952.
- [19] E. Agliari, A. Barra, A Hebbian approach to complex-network generation, *EPL* 94 (2011) 10002.
- [20] M. Uzuntarla, E. Barreto, J.J. Torres, Inverse stochastic resonance in networks of spiking neurons, *PLoS Comput. Biol.* 13 (2017) e1005646.
- [21] F. Devalle, A. Roxin, E. Montbrío, Firing rate equations require a spike synchrony mechanism to correctly describe fast oscillations in inhibitory networks, *PLoS Comput. Biol.* 13 (2017) e1005881.
- [22] T.B. Luke, E. Barreto, P. So, Macroscopic complexity from an autonomous network of networks of theta neurons, *Front. Comput. Neurosci.* 8 (2014) 145.
- [23] J. Ma, J. Tang, A. Zhang, Y. Jia, Robustness and breakup of the spiral wave in a two-dimensional lattice network of neurons, *Sci. China Phys. Mech. Astron.* 53 (2010) 672–679.
- [24] J. Karbowski, G.B. Ermentrout, Synchrony arising from a balanced synaptic plasticity in a network of heterogeneous neural oscillators, *Phys. Rev. E* 65 (2002) 031902.
- [25] M. Uzuntarla, J.J. Torres, A. Calim, E. Barreto, Synchronization-induced spike termination in networks of bistable neurons, *Neural Netw.* 110 (2019) 131–140.
- [26] M. Gosak, R. Markovič, J. Dolensek, M.S. Ruppik, M. Marhl, A. Stožer, M. Perc, Network science of biological systems at different scales: a review, *Phys. Life Rev.* 24 (2018) 118–135.
- [27] J. Ma, F. Wu, C. Wang, Synchronization behaviors of coupled neurons under electromagnetic radiation, *Int. J. Mod. Phys. B* 31 (2017) 1650251.
- [28] X. Sun, J. Lei, M. Perc, J. Kurths, G. Chen, Burst synchronization transitions in a neuronal network of subnetworks, *Chaos* 21 (2011) 016110.
- [29] H. Xie, Y. Gong, Q. Wang, Effect of spike-timing-dependent plasticity on coherence resonance and synchronization transitions by time delay in adaptive neuronal networks, *Eur. Phys. J. B* 89 (2016) 161.
- [30] F. Parastesh, H. Azarnoush, S. Jafari, B. Hatef, M. Perc, R. Repnik, Synchronizability of two neurons with switching in the coupling, *Appl. Math. Comput.* 350 (2019) 217–223.
- [31] S. Rakshit, B.K. Bera, D. Ghosh, Synchronization in a temporal multiplex neuronal hypernetwork, *Phys. Rev. E* 98 (2018) 032305.
- [32] T. Nowotny, V.P. Zhitulin, A.I. Selverston, H.D. Abarbanel, M.I. Rabinovich, Enhancement of synchronization in a hybrid neural circuit by spike-timing dependent plasticity, *J. Neurosci.* 23 (2003) 9776–9785.
- [33] S. Boccaletti, J. Kurths, G. Osipov, D. Valladares, C. Zhou, The synchronization of chaotic systems, *Phys. Rep.* 366 (2002) 1–101.
- [34] M.G. Rosenblum, A.S. Pikovsky, J. Kurths, From phase to lag synchronization in coupled chaotic oscillators, *Phys. Rev. Lett.* 78 (1997) 4193.
- [35] Y. Kuramoto, D. Battogtokh, Coexistence of coherence and incoherence in non-locally coupled phase oscillators, *Nonlinear Phenom. Complex Syst.* 5 (2002) 380–385.
- [36] D.M. Abrams, S.H. Strogatz, Chimera states for coupled oscillators, *Phys. Rev. Lett.* 93 (2004) 174102.
- [37] B.K. Bera, S. Majhi, D. Ghosh, M. Perc, Chimera states: Effects of different coupling topologies, *Europhys. Lett.* 118 (2017) 10001.
- [38] A. Buscarino, M. Frasca, L.V. Gambuzza, P. Hövel, Chimera states in time-varying complex networks, *Phys. Rev. E* 91 (2015) 022817.
- [39] D. Dudkowski, K. Czołczyński, T. Kapitaniak, Traveling chimera states for coupled pendula, *Nonlinear Dyn.* 95 (2019) 1859–1866.
- [40] F. Parastesh, S. Jafari, H. Azarnoush, B. Hatef, A. Bountis, Imperfect chimeras in a ring of four-dimensional simplified Lorenz systems, *Chaos, Solitons Fract.* 110 (2018) 203–208.
- [41] S. Majhi, B.K. Bera, D. Ghosh, M. Perc, Chimera states in neuronal networks: a review, *Phys. Life Rev.* 28 (2019) 100–121.
- [42] R.G. Andrzejak, C. Rummel, F. Mormann, K. Schindler, All together now: analogies between chimera state collapses and epileptic seizures, *Sci. Rep.* 6 (2016) 23000.
- [43] M.S. Santos, P.R. Protachevitz, K.C. Iarosz, I.L. Caldas, R.L. Viana, F.S. Borges, H.-P. Ren, J.D. Szezech Jr, A.M. Batista, C. Grebogi, Spike-burst chimera states in an adaptive exponential integrate-and-fire neuronal network, *Chaos* 29 (2019) 043106.
- [44] Z. Wei, F. Parastesh, H. Azarnoush, S. Jafari, D. Ghosh, M. Perc, M. Slavinec, Nonstationary chimeras in a neuronal network, *EPL* 123 (2018) 48003.
- [45] L. Khaleghi, S. Panahi, S.N. Chowdhury, S. Bogomolov, D. Ghosh, S. Jafari, Chimera states in a ring of map-based neurons, *Physica A* 536 (2019) 122596.
- [46] S. Kundu, B.K. Bera, D. Ghosh, M. Lakshmanan, Chimera patterns in three-dimensional locally coupled systems, *Phys. Rev. E* 99 (2019) 022204.
- [47] S. Majhi, D. Ghosh, Alternating chimeras in networks of ephaptically coupled bursting neurons, *Chaos* 28 (2018) 083113.
- [48] B.K. Bera, S. Rakshit, D. Ghosh, J. Kurths, Spike chimera states and firing regularities in neuronal hypernetworks, *Chaos* 29 (2019) 053115.
- [49] V.V. Makarov, S. Kundu, D.V. Kirsanov, N.S. Frolov, V.A. Maksimenko, D. Ghosh, S.K. Dana, A.E. Hramov, Multiscale interaction promotes chimera states in complex networks, *Commun. Nonlinear Sci. Numer. Simul.* 71 (2019) 118–129.
- [50] K. Bansal, J.O. Garcia, S.H. Tompson, T. Verstynen, J.M. Vettel, S.F. Muddoan, Cognitive chimera states in human brain networks, *Sci. Adv.* 5 (2019) eaau8535.
- [51] A. Calim, P. Hövel, M. Ozer, M. Uzuntarla, Chimera states in networks of type-I Morris-Lecar neurons, *Phys. Rev. E* 98 (2018) 062217.
- [52] M. Santos, J. Szezech, F. Borges, K. Iarosz, I. Caldas, A. Batista, R. Viana, J. Kurths, Chimera-like states in a neuronal network model of the cat brain, *Chaos, Solitons Fract.* 101 (2017) 86–91.
- [53] S. Huo, C. Tian, L. Kang, Z. Liu, Chimera states of neuron networks with adaptive coupling, *Nonlinear Dyn.* 96 (2019) 75–86.
- [54] B.K. Bera, D. Ghosh, M. Lakshmanan, Chimera states in bursting neurons, *Phys. Rev. E* 93 (2016) 012205.



**Zhen Wang** was born in Shaanxi, China, in 1981. He received the B.S. degree and M.S. degree in 2004 and 2008, respectively from Shaanxi University of Science and Technology, China. He is currently a professor of School of Science at Xijing University. His research interests include ordinary differential equations and dynamical systems, nonlinear control system theory etc.



**Sara Baruni** was born in Tabas, Iran, in 1996. She receives her B.Sc. degree in Biomedical Engineering in 2019 from Biomedical Engineering department, Amirkabir University of Technology, Tehran, Iran. Her research interest is nonlinear and chaotic signals, systems, and networks.



**Fatemeh Parastesh** was born in Tehran, Iran, in 1992. She received the B.Sc. and M.S. degrees in Biomedical Engineering from the Biomedical Engineering Department, Amirkabir University of Technology, Tehran, Iran, in 2014 and 2017, respectively. She is currently the Ph.D. student in Biomedical Engineering Department of Amirkabir University of Technology. Her research interests include nonlinear dynamics, networks, synchronization and chimera state.



**Sajad Jafari** was born in Kermanshah, Iran, in 1983. He received his B.Sc., M.S., and Ph.D. degrees in Biomedical Engineering in 2005, 2008, and 2013 from Biomedical Engineering Department, Amirkabir University of Technology, Tehran, Iran. He is currently an assistant professor in there (since 2013). His research interests include nonlinear and chaotic signals and systems and complex networks. He serves as editor in International Journal of Bifurcation and Chaos, International Journal of Electronics and Communications, and Radioengineering.



**Dibakar Ghosh** is an associate professor in the Physics and Applied Mathematics Unit, Indian Statistical Institute, Kolkata, India. He received the Ph.D. degree in Nonlinear Dynamics from the Jadavpur University, Kolkata, India, in 2009. His current research interests include nonlinear dynamical systems, complex networks, temporal networks, extreme events and machine learning.



**Iqtadar Hussain** is an assistant professor at Qatar University. He received his PhD in Mathematics, in 2014, specializing in the area of Cryptography. His current research expertise and research interests include applications of mathematical concepts in the field of secure communication and cybersecurity where he has published 80 papers in well-known journals. His h-index score is 25 and i-10 index score is 42. His articles have 1660 Google Scholar citations.



**Matjaž Perc** is Professor of Physics at the University of Maribor. He is a member of Academia Europaea and the European Academy of Sciences and Arts, and he is among top 1% most cited physicists according to Clarivate Analytics. He is also the 2015 recipient of the Young Scientist Award for Socio and Econophysics from the German Physical Society, and the 2017 USERN Laureate. In 2018 he received the Zois Award, which is the highest national research award in Slovenia. Matjaž is currently Editor at Physics Letters A, Chaos, Solitons and Fractals, EPL, and Frontiers in Physics, and he is on the Editorial Board of New Journal of Physics, Proceedings of the Royal Society A, Journal of Complex Networks, European Physical Journal B, Scientific Reports, and Royal Society Open Science.